Conformal Mesh Mappings

Bachelor Thesis D-MATH ETHZ
Alessandra Iacopino
Supervisor: Prof. Dr. Ralf Hiptmair

Abstract

Given a 2D triangular mesh $\widehat{\mathcal{M}}$ of the unit disk $\mathbb{D}$, whose triangles are all nicely shape-regular (in the sense that the ratio of their diameter to the radius of the largest inscribed circle is uniformly bounded for all triangles), we are guaranteed the existence of a conformal mapping ψ from $\mathbb{D}$ to any simply connected bounded domain Ω by the Riemann mapping theorem. This allows for a sufficiently "nice" mesh $\mathcal{M}$ on Ω to be obtained as the image of $\widehat{\mathcal{M}}$ under ψ, i.e. $\mathcal{M} = \psi(\widehat{\mathcal{M}})$. The challenge lies in the numerical construction/ approximation of this conformal mapping ψ. This text is intended to give a general overview of currently known numerical conformal mapping algorithms, and to provide a comparison in terms of accuracy, runtime, and the representation format of the resulting map, particularly emphasizing the efficiency of point evaluations for both the mapping ψ itself and its derivative (Jacobian) $D\psi$. Finally, we implement Wegmann's Method in Python.

Contents

1 Theoretical Background

Conventions

Throughout this text, we identify $\mathbb{R}^2$ with the complex plane $\mathbb{C}$ and write

$$\mathbb{C} \ni z = x + iy \text{ where } x, y \in \mathbb{R}.$$

The task is to find an angle-preserving mapping ψ from the unit disk $\mathbb{D}$ to Ω, given a simply connected bounded domain $\Omega \subset \mathbb{C}$ with boundary Γ and 2π-periodic parametrization

$$\eta : [0, 2\pi] \to \Gamma \quad \text{with} \quad \eta \in C^0([0, 2\pi])$$

by its fourier series representation. In particular, for the implementation we are given a matrix of size $N \times 2$ containing $2N$ complex fourier coefficients, thus our boundary is parametrised by a trigonometric polynomial and hence smooth.

We are also given a curvilinear triangular mesh $\widehat{\mathcal{M}}$ on $\mathbb{D}$ satisfying some regularity conditions (see chapter 1.6).

Definition 1
We call a subset $\Omega \in \mathbb{C}$ **proper** if $\emptyset \neq \Omega \neq \mathbb{C}$.

1.1 Conformal Mappings

Definition 2
A **conformal mapping**, also called a conformal map, conformal transformation, angle-preserving transformation, or biholomorphic map, is a transformation $f(z)$ that preserves local angles. An analytic function is conformal at any point where it has nonzero derivative.

Definition 3
A **complex analytic function** or **holomorphic function** on an open subset $U \subset \mathbb{C}$ is locally given by a convergent power series, i.e. for any $z_0 \in U$ there exists a neighborhood $V \subset U$ of z_0 such that for all $z \in V$ we have

$$f(z) = \sum_{n=0}^{\infty} a_n (z - z_0)^n$$

for some complex coefficients $a_n \in \mathbb{C}$. The terms analytic and holomorphic are used interchangeably.

1.2 Riemann Mapping Theorem

Theorem 1.1 (Riemann Mapping Theorem)
If Ω is a non-empty simply connected open proper subset of the complex plane $\mathbb{C}$, then there exists a biholomorphic mapping f (i.e. a bijective holomorphic mapping whose inverse is also holomorphic) from Ω onto the open unit disk

$$\mathbb{D} = \{z \in \mathbb{C} : |z| < 1\}.$$

This mapping is known as a Riemann mapping.

The beauty of the Riemann mapping theorem lies in its weight of implications, i.e. the fact that it guarantees the existence of a conformal map between any two simply connected domains in the complex plane, provided they are not the entire plane. The existence of this Riemann map is a priori not obvious: Even relatively simple Riemann mappings (for example a map from the interior of a circle to the interior of a square) have no explicit formula using only elementary functions [Weg05]. Simply connected open sets in the plane can be highly complicated, for instance, the boundary can be a nowhere-differentiable fractal curve of infinite length, even if the set itself is bounded. One such example is the Koch curve. The fact that such a set can be mapped in an angle-preserving manner from the nice and regular unit disc seems counter-intuitive.

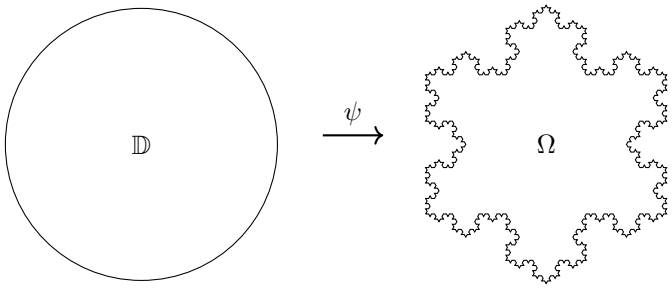

We closely follow the proof by normal families in [SS03].

1.2.1 Preliminary Results

Lemma 1.2 (Schwarz Lemma [SS03, Lemma 2.1])
Let $f : \mathbb{D} \to \mathbb{D}$ be holomorphic with $f(0) = 0$. Then

1. $|f(z)| \leq |z|$ for all $z \in \mathbb{D}$.
2. If for some $z_0 \neq 0$ we have $f(z_0) = z_0$ then f is a rotation.
3. $|f'(0)| \leq 1$ and if equality holds, then f is a rotation.

Definition 4 ([SS03, page 225])
A family $\mathcal{F}$ of holomorphic functions on a domain Ω is called **normal** if every sequence in $\mathcal{F}$ contains a subsequence that converges uniformly on any compact subset of Ω.

Definition 5 ([SS03, page 225])
A family $\mathcal{F}$ is called **uniformly bounded on compact subsets** of Ω if for every compact subset $K \subset \Omega$ there exists a constant M_K such that $|f(z)| \leq M_K$ for all $z \in K$ and all $f \in \mathcal{F}$.

Definition 6 ([SS03, page 225])
A family $\mathcal{F}$ of holomorphic functions on a domain Ω is called **equicontinuous** if for every $\varepsilon > 0$ there exists a $\delta > 0$ such that if $z \in \Omega$ with $|z - z_0| < \delta$ we have $|f(z) - f(z_0)| < \varepsilon$ for all $f \in \mathcal{F}$.

Theorem 1.3 (Montel [SS03, Theorem 3.3])
A family $\mathcal{F}$ of holomorphic functions on Ω that is uniformly bounded on compact subsets of Ω is normal if and only if it is equicontinuous on compacta.

Theorem 1.4 (Hurwicz [Wik25c])
Let $\Omega \subset \mathbb{C}$ be a connected open subset and let $f_n : \Omega \to \mathbb{C}$ be a sequence of injective holomorphic functions that converges uniformly on compact subsets of Ω to a holomorphic function $f \neq 0$. If f has a zero of order m at z_0 then for every $\varepsilon > 0$ and sufficientlly large $k = k(\varepsilon) \in \mathbb{N}$, f_k has precisely m zeros in $B_\varepsilon(z_0)$ including multiplicities. Moreover, the zeros converge to z_0 as $k \to \infty$.

We will use the following corollary of Hurwicz' theorem in the proof of 1.1:

Corollary 1.5 ([SS03, Proposition 3.5])
Let $\Omega \subset \mathbb{C}$ be a connected open subset and let $f_n : \Omega \to \mathbb{C}$ be a sequence of injective holomorphic functions that converges uniformly on compact subsets of Ω to a holomorphic function f. Then f is either constant or injective.

Proposition 1.6 (Cauchy Inequality [SS03, Corollary 4.3])
Let f be holomorphic on an open set containing the closure of a ball $B_R(z_0)$ centered at z_0 of radius R. Then

$$|f^{(n)}(z_0)| \leq \frac{n! \|f\|_R}{R^n},$$

where $\|f\|_R = \sup_{\|z\|=R} |f(z)|$ on the boundary circle $\partial B_R(z_0)$.

Theorem 1.7 (Maximum Modulus Principle [SS03, Theorem 4.5])
Let $\Omega \subset \mathbb{C}$ be a connected open bounded set and $f : \Omega \to \mathbb{C}$ holomorphic. If z_0 is a point in Ω such that $|f(z_0)| \geq |f(z)|$ for all z in a neighborhood of z_0, then f is constant on Ω.

Theorem 1.8 (Implicit Mapping Theorem [EW22, Theorem 12.1])
Let $r > 0$ be a radius, and let $x_0 \in \mathbb{R}^n$, $y_0 \in \mathbb{R}^m$. Consider the open set $W = B_r(x_0) \times B_r(y_0) \subset \mathbb{R}^n \times \mathbb{R}^m$ defined as

$$W = \{(x, y) \in \mathbb{R}^n \times \mathbb{R}^m : \|x - x_0\|_2 < r \text{ and } \|y - y_0\|_2 < r\}.$$

Let $F : W \to \mathbb{R}^m$ be a continuous function satisfying the following conditions:

1. $F(x_0, y_0) = 0$.
2. The partial derivatives $\partial_{y_k} F : W \to \mathbb{R}^m$ exist for all $k \in \{1, \ldots, m\}$ and are continuous on W.

3. The partial differential $D_yF(x_0, y_0)$ (the differential of the map $y \mapsto F(x_0, y)$ at y_0) is invertible.

Then there exist radii $\alpha, \beta \in (0, r)$ such that for the open balls $U_0 = B_\alpha(x_0) \subset \mathbb{R}^n$ and $V_0 = B_\beta(y_0) \subset \mathbb{R}^m$, there exists a unique continuous function $f : U_0 \to V_0$ satisfying:

- $f(x_0) = y_0$.
- $\forall (x, y) \in U_0 \times V_0 : F(x, y) = 0 \quad \iff \quad y = f(x)$.

1.2.2 Proof of Riemann Mapping Theorem

Step 1: Existence and injectivity
Let Ω be a simply connected open proper subset of $\mathbb{C}$. We show that Ω is conformally equivalent to an open subset of the unit disk containing the origin. Indeed, choose $\alpha \notin \Omega$ and consider the function

$$f(z) := log(z - \alpha)$$

on Ω, which is well-defined and holomorphic since $z - \alpha$ never vanishes on Ω. Note f is injective since $e^{f(z)} = z - \alpha$ is $(f(z_1) = f(z_2) \implies z_1 - \alpha = z_2 - \alpha)$. Then for a point $\omega \in \Omega$ we get $f(z) \neq f(\omega) + 2\pi i \quad \forall z \in \Omega$ since otherwise we would find $z = \omega$ again by exponentiating. In fact, $f(z) \cap B_\varepsilon(f(\omega) + 2\pi i) = \emptyset$ for some $\varepsilon > 0$ since otherwise we would find a sequence $z_n \to \omega$ with $f(z_n) \to f(\omega) + 2\pi i$, contradicting the continuity of f. Finally, the function

$$g(z) := \frac{1}{f(z) - (f(\omega) + 2\pi i)}$$

is well-defined, holomorphic and injective on Ω and maps Ω to a bounded subset $g(\Omega) \subset \mathbb{C}$, so g is conformal. By boundedness of $g(z) < \frac{1}{\varepsilon}$ we can scale and translate $g(\Omega)$ to contain the origin and fit into the unit disk.

Step 2: Existence of the extremal function, aka the maximum is attained
By step 1 we can assume Ω to be an open subset of the unit disk with $0 \in \Omega$. Consider the family

$$\mathcal{F} := \{f : \Omega \hookrightarrow \mathbb{D} \text{ holomorphic}, \ f(0) = 0\}$$

of all injective holomorphic functions which map the origin to itself. Note that $\mathcal{F} \neq \emptyset$ since it contains the identity, and it is a uniformly bounded family by construction (maps into, hence bounded by the unit disk). In order to use the Hurwicz corollary and get injectivity, we now want to find a function $f_M \in \mathcal{F}$ that maximizes $|f'(0)|$ (to rule out constant functions yielded otherwise by the application of said corollary). Observe that by the Cauchy inequality 1.6, the derivatives $|f'(0)|$ are uniformly bounded for all f in $\mathcal{F}$. Thus, we can define

$$s := \sup_{f \in \mathcal{F}} |f'(0)|.$$

and choose a sequence $f_n \subset \mathcal{F}$ such that $|f_n'(0)| \to s$ as $n \to \infty$. By Montel's theorem, f_n has a subsequence converging uniformly on compacta to a holomorphic f_M on Ω. Since $s \geq 1$ (the identity is in $\mathcal{F}$), f_M is non-constant. Hence by the Hurwicz corollary 1.5, f_M must be injective. By continuity we have $|f_M(z)| \leq 1$ for all $z \in \Omega$, and since f_M is non-constant, by the Maximum Modulus Principle 1.7 we get $|f_M(z)| < 1$. Finally and since $f_M(0) = 0$, we have $f_M \in \mathcal{F}$ and $|f_M'(0)| = s$.

Step 3: Surjectivity
By injectivity it suffices to show f_M is surjective. Suppose towards a contradiction that f_M is not surjective, we will construct a function in $\mathcal{F}$ with derivative greater than s at the origin.

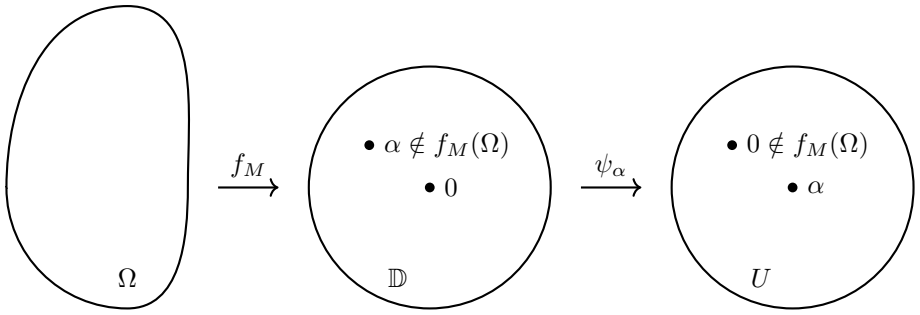

So let $\alpha \in \mathbb{D}$ be such that $\alpha \notin f_M(\Omega)$ and consider the automorphism of the unit disk that interchanges 0 and α,

$$\psi_\alpha(z) := \frac{\alpha - z}{1 - \bar{\alpha} z}.$$

Since Ω is simply connected and f_M and $\psi_\alpha(\Omega)$ are continuous, the set

$$U := (\psi_\alpha \circ f_M)(\Omega)$$

is simply connected and does not contain the origin. Thus we can define a square root function on U by

$$q(w) := e^{\frac{1}{2} log w}.$$

Next, consider the function $F := \psi_{q(\alpha)} \circ q \circ \psi_\alpha \circ f_M$.

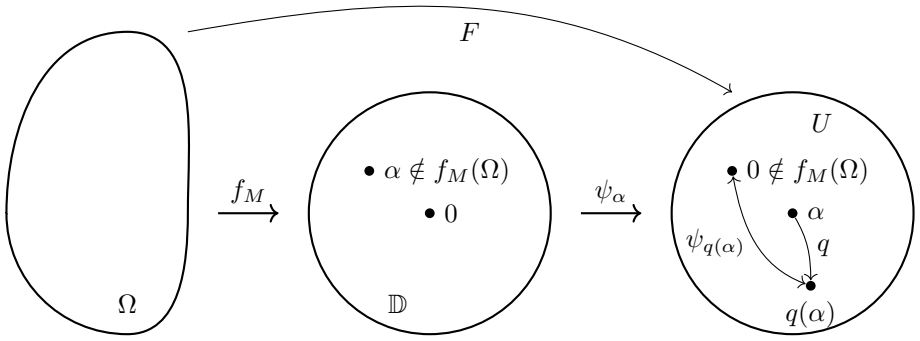

Then $F \in \mathcal{F}$ since $F(0) = 0$ and F is holomorphic and injective since all the composing functions are. Also, F maps into the unit disk since all the composing functions do. But now if h denotes the square function $h(w) = w^2$, then we must have

$$f_M = \psi_\alpha^{-1} \circ h \circ \psi_{q(\alpha)}^{-1} \circ F = \phi \circ F.$$

But $\phi : \mathbb{D} \to \mathbb{D}$ satisfies $\phi(0) = 0$ and is not injective since F is but h is not. By the Schwarz lemma 1.2 we get $|\phi'(0)| < 1$ and hence

$$|f_M'(0)| = |\phi'(0)||F'(0)| < |F'(0)|,$$

contradicting maximality of $|f_M'(0)|$ in $\mathcal{F}$.

Finally, multiplying f_M with a suitable unimodular complex number gives the desired conformal map $\psi : \Omega \to \mathbb{D}$ with

$$\psi(0) = 0, \quad \psi'(0) > 0. \tag{1}$$

□

Note that the Riemann mapping is unique up to three real degrees of freedom, which are fixed by setting (1) in the above proof. Later the uniqueness will be achieved by prescribing the image of three distinct boundary points instead, as we will only be working with the boundaries.

Corollary 1.9
Any two simple connected open proper subsets of $\mathbb{C}$ are conformally equivalent.

Proof. This follows directly from the Riemann mapping theorem by taking the unit disk as an intermediate step. □

Theorem 1.10 (Carathéodory [Pom92, Theorem 2.6], [Weg05, Theorem 3])
The conformal mapping $\psi : \mathbb{D} \to \Omega$ can be extended to a continuous mapping $\psi : \bar{\mathbb{D}} \to \bar{\Omega}$ if and only if the boundary $\Gamma = \partial\Omega$ consists of a Jordan curve.

Existence established, the problem now becomes the explicit construction of a conformal mapping. Once the boundaries of the domain and target region

are conformally mapped, the interior can be deduced from the boundary by the Cauchy Integral Formula [Weg05, page 357], [Gai64, Theorem 1.2]

$$\psi(z) = \frac{1}{2\pi i} \int_{\partial\mathbb{D}} \frac{\psi(\zeta)}{\zeta - z} d\zeta \quad \text{for } z \in \mathbb{D}. \tag{2}$$

Hence why the main focus of the task lies on mapping boundary to boundary.

1.3 Reformulation as Boundary Value Problem

When the region Ω is bounded by a closed Jordan curve Γ the mapping

$$\psi : \mathbb{D} \to \Omega$$

can be extended continuously to the closure $\overline{\mathbb{D}}$ by Carathéodory's Extension Theorem 1.10. Assume the boundary to be parametrized by a 2π-periodic function η in counterclockwise direction (positive orientation, aka *normal representation* [Weg05, page 387]) and the mapping ψ to be determined by its boundary values

$$\psi(e^{it}) = \eta(S(t)) \quad \text{for } t \in [0, 2\pi). \tag{3}$$

S is called the **boundary correspondence function**. By the Riemann mapping theorem, we need to fix at least three degrees of freedom (1) for uniqueness of the conformal mapping ψ, which we achieve through fixing three points on the boundary via the boundary correspondence equation (3).

From Definition 2 we know that a complex differentiable function with non-vanishing complex derivative is conformal, and complex differentiability in two dimensions can be caracterised by the Cauchy-Riemann equations (necessary and sufficient condition). Denoting $z = x + iy$ and

$$J := \begin{pmatrix} \partial_x & -\partial_y \\ \partial_y & \partial_x \end{pmatrix}$$

we want to find a deformation $\psi(z) = \psi(x + iy) = u + iv$ such that $J\psi = 0$.

Definition 7 ([Hen86, §15.1])
A function $f : \mathbb{C} \supseteq \Omega \to \mathbb{C}$ is called **harmonic** in Ω if it has continuous second partial derivatives and

$$\Delta f := \frac{\partial^2 f}{\partial x^2} + \frac{\partial^2 f}{\partial y^2} = 0 \quad \forall z = x + iy \in \Omega.$$

As a byproduct of the Cauchy-Riemann equations, both components of a conformal map are harmonic functions, i.e. they satisfy Laplace's equation $\Delta u = 0 = \Delta v$. Thus, one way to construct conformal maps is to solve Laplace's equation with suitable boundary conditions.

Definition 8 ([Hen86, §13.5])
Two harmonic functions $u(x, y)$ and $v(x, y)$ on a domain are called **conjugate** if they satisfy the Cauchy-Riemann equations on the domain. E.g. v is a conjugate for u, and $-u$ is a conjugate for v.

This directly leads to the conclusion that it suffices to find only one of the components of $\psi = u + iv$, since the other one can then be deduced as its conjugate harmonic function. This formulation is called the **Dirichlet problem** for the Laplace equation. It can be described as finding ψ analytic in $\mathbb{D}$, continuous in $\overline{\mathbb{D}}$ and satisfying

$$\begin{array}{ll} u(e^{it}) = Re(\psi(e^{it})) = \eta(S(t)) & \text{on } \partial\mathbb{D} \\ \Delta u = 0 & \text{in } \mathbb{D}^\circ, \end{array} \tag{4}$$

where ψ is 2π-periodic and Hölder continuous [Weg05, Chapter 12.3]. This problem has a unique real solution u, which then yields a unique solution for ψ up to an additive imaginary constant [Hen86, Corollary 15.1b](which we fix via our normalisation condition (1)), which can be constructed using the conjugation operator

$$K\psi(s) := \frac{1}{2\pi} \int_0^{2\pi} \psi(t) \cot(\frac{s-t}{2}) dt, \tag{5}$$

which is also known as Hilbert Transform (details on this in [CR25]).

Remark 1 ([Weg05, Chapter 12.3])
In order to implement numerical methods efficiently via the Fast Fourier Transform later, we will use the functions' Fourier series representations. Hence e.g. on a grid of $N = 2n$ equidistant points $t_j = \frac{(j-1)2\pi}{N}$, ψ will be written as

$$\psi(t_j) = \sum_{k=-n+1}^{n} c_k e^{ikt_j} \text{ for } j \in [N]$$

and the conjugation operator can be approximated by the operator K_N defined as

$$K_N\psi(t_j) = \sum_{k=1}^{n-1} -ic_k e^{ikt_j} + ic_{-k} e^{-ilt_j}.$$

The function K_N is thus defined as a trigonometric polynomial obtained by interpolating ψ at the grid points. This approximation of the actual operator K satisfies

$$\|K\psi - K_N\psi\|_\infty \in O(n^{-\alpha+1/2})$$

for $\psi \in C^\alpha$ Hölder continuous. If ψ is smoother, e.g. $\psi \in C^{k-1}$, the error decreases to

$$\|K\psi - K_N\psi\|_\infty \in O(n^{-k} \log(n) \|\psi^{(k)}\|_\infty).$$

These considerations are of particular importance for all methods based on conjugation.

In principle, there are two strategies for finding conformal mappings, namely to solve linear or non-linear boundary value problems. The linear problems are naturally faster to solve numerically, however their kernels must be adapted to

each new fixed boundary and thus these methods present complications when dealing with predefined boundaries. Non-linear methods on the other hand can be more flexible with respect to the boundary shape, but are computationally more expensive. But since we are mainly interested in solving the mapping problem for a fixed boundary shape, we will focus on linear methods in this article.

1.4 Boundary Conditions

Remark 2 (citation)
Note that the Cauchy-Riemann equations do not guarantee a solution for arbitrary boundary data. A holomorphic map from the boundary of the unit disk onto some boundary of a convex set in $\mathbb{C}$ satisfies Cauchy-Riemann equations if the boundary of the target set can be described by non-negative Fourier frequencies. Thus, the choice of parametrization of the target region's boundary is usually another challenge posed when solving conformal mapping problems, but for the scope of this article we assume to be given a suitable parametrization of $\partial\Omega$.

1.5 Solution of the Boundary Value Problem via Fredholm Integral Equations of the Second Kind

We often numerically solve BVPs by transforming them into integral equations [Hen86, page 281]. Integral equations are equations in which an unknown function appears under an integral sign. They are classified into two main types: Fredholm and Volterra integral equations, where Fredholm integral equations have fixed limits of integration, while Volterra integral equations have variable limits of integration. Both types can be further categorized into first kind and second kind, depending on whether the unknown function appears only under the integral sign or also outside of it [Wik25b].

Definition 9
A **Fredholm integral equation of the second kind** is an equation of the form

$$f(x) = \lambda \int_a^b K(x,t)\psi(t)dt + \psi(x) \tag{6}$$

where f is a known function, ψ is the unknown function to be solved for, $K(x,t)$ is a given kernel function, $\lambda \in \mathbb{R}$ is a constant, and $x, a, b \in \mathbb{R}$, $a \leq b$.

There are several methods to solve Fredholm integral equations of the second kind, which we will explore in what follows.

1.5.1 Neumann Kernel

The Neumann kernel is named after Carl Neumann, who first introduced it as a tool for solving Integral equations corresponding to the Dirichlet problem

[Gai64, §1.1c]. Let $\eta : [0, 2\pi] \to \Gamma$ be a parametrization of the boundary and $s, t \in [0, 2\pi]$. Consider the straight line segment from $\eta(t)$ to $\eta(s)$ and denote by r_{st} its length. Moreover, let $\theta(t), \theta(s)$ denote the tangent angles (measured with regard to the positive real axis) to η at s, t respectively, and $\phi(s), \phi(t)$ the angles between the positive real axis and the line from the origin to $\eta(s), \eta(t)$ respectively.

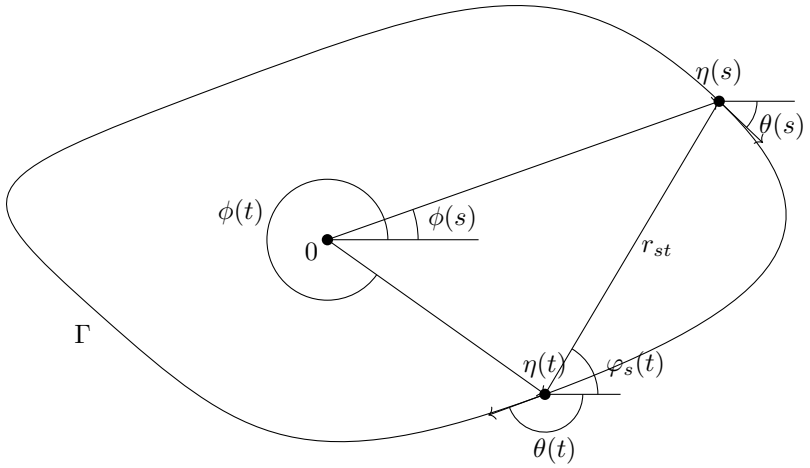

The Neumann kernel is defined for $s \neq t$ as

$$K(s,t) = \frac{1}{\pi} \frac{\sin(\theta(t) - \varphi_s(t))}{r_{st}} \tag{7}$$

Remark 3 ([Gai64, page 40])
The integral in equation (6) can be interpreted as a Riemann or Riemann-Stieltjes integral, where the latter is more general and allows for evaluation of non-bounded integrands. This could be important if the boundary correspondence function S as seen in (3) is not continuously differentiable. These two interpretations lead to different methods of discretisation and different error estimates when solving the integral equation numerically. However, since we will only be working with smooth boundaries in this article, we will not go into further detail on this topic.

1.6 Discretisation

In order to numerically solve boundary value problems the domain is usually discretised by creating a mesh $\mathcal{M}$ of N nodes (points) and M elements (cells) covering the domain Ω. There are many methods to create such meshes, but for the scope of this article we will assume to be given a mesh on the domain

and only briefly discuss some important properties of meshes and mesh generation methods. We highly recommend referring to [Bro90] for a more in-depth treatment of mesh generation techniques.

Definition 10 ([Hip23, Definition 2.5.1.1])
A **mesh** on $\Omega \in \mathbb{C}$ is a finite collection $\mathcal{M} := \{K_i\}_{i\in[M]}, M \in \mathbb{N}$ of open non-degenerate (curvilinear) polygons called **cells** such that

1. $\overline{\Omega} = \bigcup_{i\in[M]} \overline{K_i}$,
2. $K_i \cap K_j = \emptyset \iff i \neq j$,
3. $\forall i \neq j \in [M] : \overline{K_i} \cap \overline{K_j} \in \begin{cases} \emptyset, \\ \text{a common vertex of both cells or} \\ \text{a common edge of both cells} \end{cases}$

In two dimensions, the most common choice for mesh elements are triangles or quadrilaterals. Triangular meshes are more flexible in adapting to complex geometries, while quadrilateral meshes can provide better accuracy for certain types of problems. Hybrid meshes combining both types are also used in practice to combine advantages.

We will be given a triangular mesh in the form of a list of nodes and a list of cells by two vectors: A $N \times 2$ matrix of points (complex coordinates of N nodes) and a $M \times 3$ matrix of integers (containing the indices of nodes constituing each of the M triangles).

1.6.1 Mesh Structure

To ensure bijectivity and conformality of the mapping ψ acting on the discretised domain, the discretisation must be done intelligently, i.e. the mesh must satisfy certain regularity criteria. Ill-chosen meshes could lead to overlaps of the target mesh nodes, failing bijectivity, or even non-conformality of ψ due to the failure to satisfy the discrete geometric constraints which are required for angle preservation.

In order to keep the approximation error as low as possible while maintaining good solver performance, we typically want uniform meshes, e.g. where the triangulation is close to equilateral. The quality of a mesh is measured in terms of its individual cells [Wec19, §4.1] where for a mesh $\mathcal{M} := \{K\}$ of triangles K such that

$$\overline{\Omega} = \cup_{K\in\mathcal{M}} K \tag{8}$$

we define $d(K)$ the diameter of the smallest K-circumscribing ball (aka diameter of K) and $\mu(K)$ the diameter of the largest ball inscribed in K. Then a measure for the quality of K is the ratio of these diameters

$$\rho(K) := \frac{d(K)}{\mu(K)} \in [1, \infty). \tag{9}$$

to do. add a mesh quality analyser to the code

1.7 Crowding AKA the Geneva Effect

Crowding is the phenomenon that occurs when a set of more or less equally distributed points on the domain are mapped to a much more dense set of points on the target region, thereby causing numerical issues due to the angles on the grid becoming very small [Gai64,], [Hen86, page 428], [Ban08]. This typically occurs when the target region is elongated, i.e. has a high aspect ratio. The following illustration shows the concentration of points near the equator of the ellipse when mapping equidistant points from the unit disk.

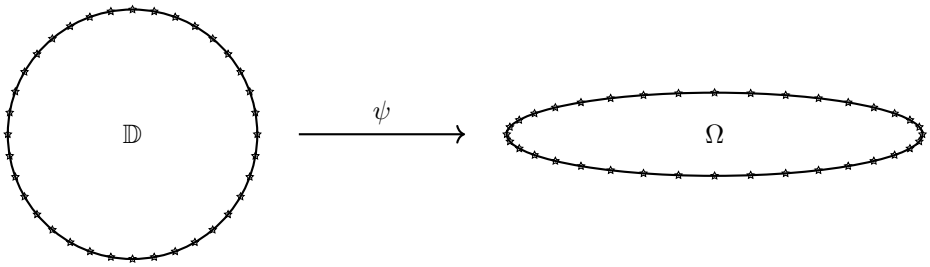

Wegmann proved the following result.

Theorem 1.11 ([Weg05, Theorem 6])
When the region G can be enclosed in a rectangle with sides a and b, $b \leq a$, such that G touches both small sides then the conformal mapping $\psi : \mathbb{D} \to \Omega$ satisfies

$$\|\psi'\|_D \geq b\psi(b/a)$$

with a function $\psi(\tau)$ which behaves for small τ like

$$\psi(\tau) \approx \frac{1}{2\pi\sqrt{\epsilon}} \exp\left(\frac{\pi}{2\tau}\right).$$

This means that crowding increases exponentially with the aspect ratio of the target region.

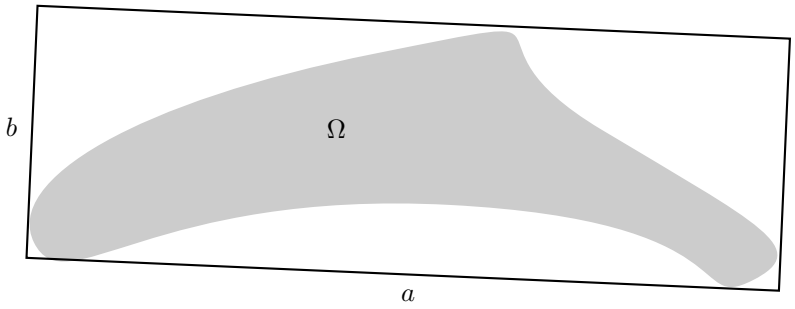

DeLillo has shown how crowding affects the accuracy of numerical computations. [DeL94]

2 Existing Methods

This chapter aims to give an overview and compare some existing methods in terms of input/output format, requirements on the boundary or shape of the regions, computational complexity, numerical stability and mesh quality preservation/ accuracy. The list is non-exhaustive but covers some of the most well-known and widely used methods.

We start with an overview of the methods covered and how to choose between them depending on the application before explaining each of them in more detail.

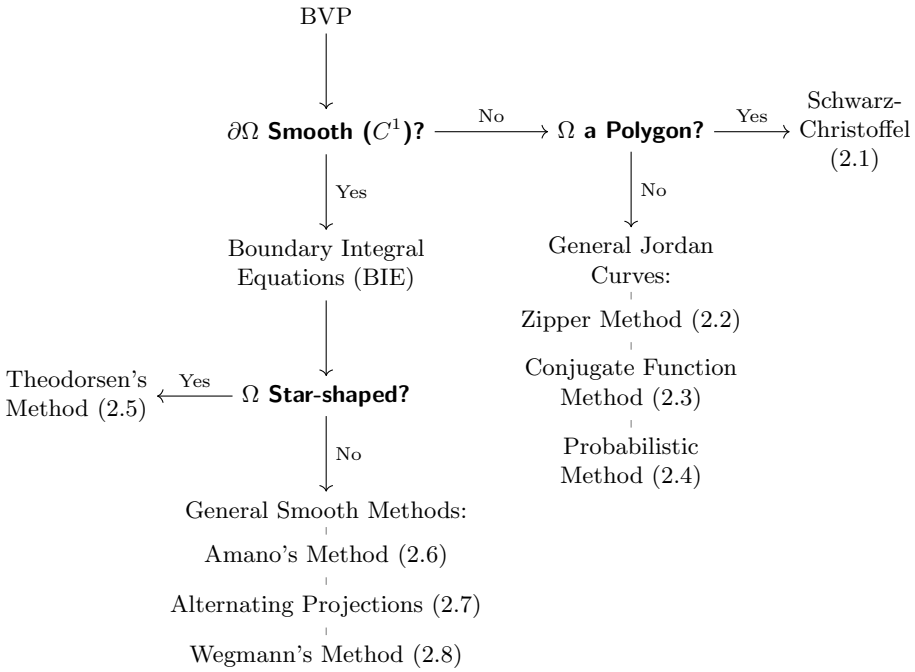

2.1 Schwarz-Christoffel Method

One class of methods for finding the conformal mapping ψ is given by the Schwarz-Christoffel equation, which relates the derivative of ψ to an integral over the boundary of the target domain Ω when Ω is a polygon.

2.1.1 Preliminaries and Notation

Definition 11 ([Wik25e])
A **Polygon** is a piecewise linear Jordan curve with finitely many line segments connecting corner points $z_1, ..., z_N$.

For each $z_i \in \Gamma$, denote the exterior angle by $\measuredangle z_i = \theta_i \pi$. Then for any polygon we have

$$\sum_{i=1}^{k} \theta_i = 2$$

and we set $\theta_i \in [-1, 1] \forall i$. Note also that P need not be bounded, since we can add vertices at complex infinity with exterior angles ranging from $[1, 3]$. These angles are defined to be 2π minus the external angle formed in the plane by the two lines meeting at infinity [Tre80].

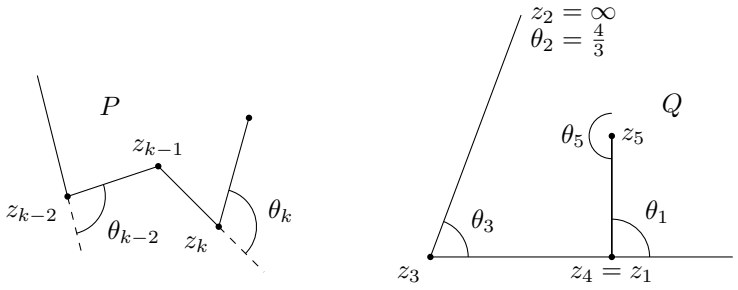

In the above example Q we have the two lines joining at z_3 again joining at infinity (z_2), where their outer angle is $\theta_2 = 2 - \theta_3 = \frac{5}{3}$, and thus the angles are

$$\theta_1 = \frac{1}{2}, \theta_2 = \frac{5}{3}, \theta_3 = \frac{1}{3}, \theta_4 = \frac{1}{2}, \theta_5 = -1 \implies \sum_{i=1}^{5} \theta_i = 2.$$

Now pick prevertices $v_1, ..., v_N \in \partial\mathbb{D}$ as well as two constants $z_c, C \in \mathbb{C}$ (these choices will be explained later) and consider the Schwarz-Christoffel formula:

$$z = \psi(v) = z_c + C \int_0^v \prod_{k=1}^{N} (1 - \frac{\zeta}{v_k})^{-\theta_k} d\zeta \tag{10}$$

Note that $1 - \frac{\zeta}{v_k} \in \{|z - 1| < 1\}$ for $|v| < 1$. Hence we can define a branch of logarithm with branch cut along the negative real axis and define $(1 - \frac{\zeta}{v_k})^{-\theta_k} = exp(-\theta_k \log(1 - \frac{\zeta}{v_k}))$, $\psi(v)$ defines an analytic function on $\mathbb{D}$ which is continuous except at the vertices v_k. The formula is constructed such that the angles at the vertices correspong precisely to the exterior angles we need, hence the image of ψ is a polygon with the correct angles. However, the lengths of the line segments need not be correct: This is where the choice of parameters $v_1, ..., v_N, z_c$ and C comes in, and this is where the computational challenge in this method lies. For the mapping to be unique, we can fix three of these parameters arbitrarily according to the Riemann mapping theorem. The remaining parameters are determined by solving the so-called **parameter problem**, which consists of a system of nonlinear equations obtained by enforcing the side lengths of the polygon to be correct.

For fixing of the initial three parameters one has two options in principle:

1. Fix three of the prevertices v_k on the unit circle.
2. Fix only one prevertex and the point $z_c = \psi(0) \in P$.

The first option results in a remaining system of size $(N-3) \times (N-3)$ which is computationally more attractive, but may be too restrictive when scaling to polygons with many more vertices, as it can lead to very uneven distribution of the prevertices on the unit circle. Hence why the second option is often preferred, even though it means solving a $(N-1) \times (N-1)$ system [Tre80, page 84]. Note that the Schwarz-Christoffel formula guarantees correctness of the angles and the prevertices are on the unit circle, hence defined by their angle; thus, it remains to tune lengths only, and our system of equations is actually real!

Thus, the first step is to fix $v_N = 1 \in \mathbb{D}$ (1 real degree of freedom) and $z_c \in P$ (two real degrees of freedom) the image of the origin under ψ. This yields uniqueness of the mapping.

Next, the scaling factor C is defined by the formula

$$\psi(v_N) - \psi(0) = z_N - z_C = C \int_0^{v_N=1} \prod_{k=1}^{N} (1 - \frac{\zeta}{v_k})^{-\theta_k} d\zeta \tag{11}$$

i.e. it is chosen such that the image of the segment from v_N to the origin is correctly scaled to match the segment from z_N to z_c. Then a first vertex is pinned down to fix the "orientation" of the polygon (rotation anchoring):

$$z_1 - z_C = C \int_0^{v_1} \prod_{k=1}^{N} (1 - \frac{\zeta}{v_k})^{-\theta_k} d\zeta \tag{12}$$

This defines two real constraints, hence it remains to formulate $N-3$ equations for our $(N-1) \times (N-1)$ system.

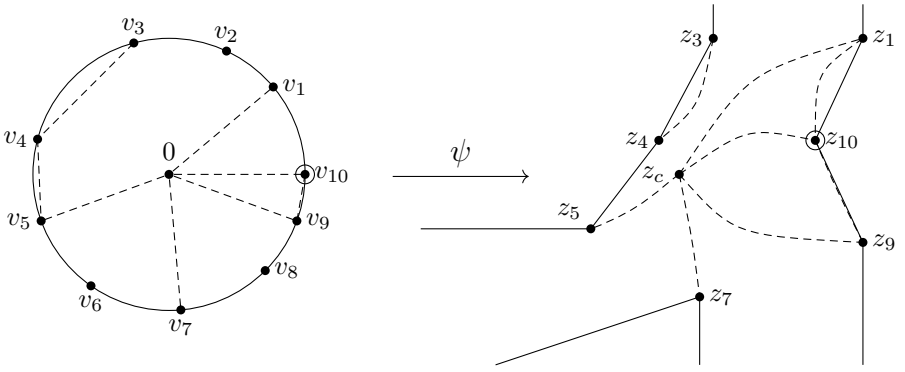

These are found by enforcing the side lengths of the polygon to be correct between the remaining vertices.

$$|z_{i+1} - z_i| = |C \int_{v_i}^{v_{i+1}} \prod_{k=1}^{N} (1 - \frac{\zeta}{v_k})^{-\theta_k} d\zeta| \quad \forall i \in 2, ..., N-2 \tag{13}$$

Note that unboundedness of the polygon is not a problem, since it can be modeled by one vertex as described earlier (2.1.1), which can be chosen to be z_N without loss of generality; this way, it will be taken care of by the first equation (11) and will not pose a problem when comparing lengths in (13).

2.2 Zipper Method

This algorithm was found independently by Kühnau and Marshall in the 1980's and has the advantage of finding ψ and its inverse at the same time. The computed map is only approximately conformal, and is obtained as a composition of conformal maps onto slit halfplanes. Depending on the shape of the slits, the Zipper algorithm looks a bit different. In this section we will focus on the easiest version called the "geodesic algorithm" [MR06]. First, let us introduce the following definition:

2.2.1 Möbius Transforms

Definition 12 ([Wik25d], [SS03, page 209])
A **Möbius transform** is a function on the extended complex plane $\hat{\mathbb{C}} := \mathbb{C} \cup \{\infty\}$ which is uniquely determined by where it sends three points. It has the form

$$f(z) = \frac{az + b}{cz + d}$$

with complex numbers a, b, c, d such that $ad - bc \neq 0$.

More explicitly, given three distinct points $z_1, z_2, z_3 \in \mathbb{C}$ and three distinct points $w_1, w_2, w_3 \in \mathbb{C}$ there exists a unique Möbius transform f such that $f(z_i) = w_i$ for $i = 1, 2, 3$:

$$f(z) = \frac{(z - z_1)(z_2 - z_3)}{(z - z_3)(z_2 - z_1)}$$

In particular, Möbius transforms are conformal and more general than affine maps, since they can e.g. map ∞ to 0 and vice versa.

2.2.2 The Geodesic Algorithm

The most elementary version of this algorithm is based on a function

$$f_a : \mathbb{H} \setminus \gamma \to \mathbb{H}$$

where $\mathbb{H}$ is the upper half plane and γ is a circular arc from 0 to $a \in \mathbb{H}$ which is orthogonal to the real axis. The orthogonal circle also meets the real axis again at $b = |a^2|\mathrm{Im}(a)$. Then the map can be expressed in closed form as

$$f_a(z) = \sqrt{g_a \circ h_a(z)}$$

where $g_a(z) = z^2 + c^2$, $c = \frac{|a^2|}{\mathrm{Im}(a)}$ is called the **conformal capacity** of γ and $h_a(z) = \frac{z}{1 - z/b}$.

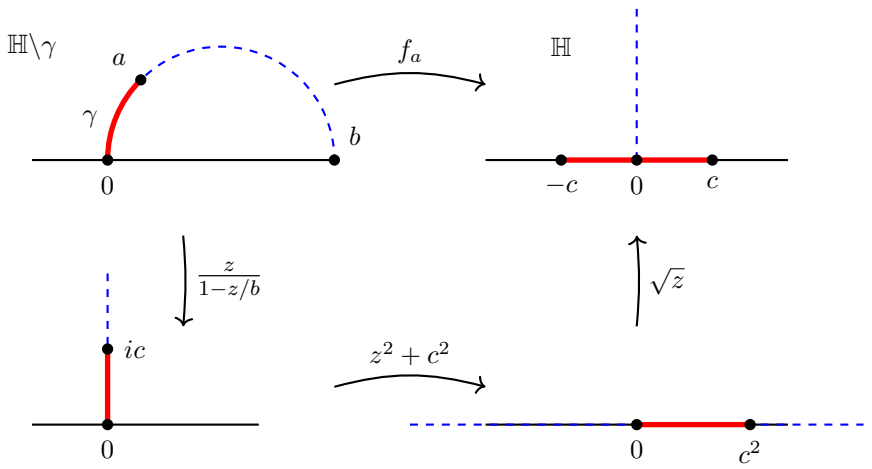

Now suppose $z_0, z_1, ..., z_n$ are points arranged counterclockwise on a Jordan curve Γ in the upper half plane. The geodesic algorithm basically iterates over the arcs from z_i to z_{i+1} and "unzips" them one by one using the map f_{a_i} where a_i is the image of z_{i+1} under the composition of all previous maps. The original geodesic algorithm proposed by Marshall and Rohde constructs a conformal map from the upper half plane to the region bounded by Γ, but it can be adapted to map from the unit disk as well via a Möbius transformation mapping the half plane to the unit disk and back first.

Algorithm 1 Geodesic Zipper Algorithm

Input: Points $z_0, z_1, ..., z_n$ on a Jordan curve Γ in the upper half plane.
Output: ψ: conformal map from $\mathbb{H}$ to the region bounded by Γ and its inverse ψ^{-1}.
$\varphi_1(z) := i\sqrt{(z-z_1)/(z-z_0)}$
$\zeta_2 := \varphi_1(z_2)$
$\varphi_2(z) := f_{\zeta_2}(z)$
for k in n **do**
  $\zeta_k := \varphi_{k-1} \circ \ldots \circ \varphi_1(z_k)$
  $\varphi_k(z) := f_{\zeta_k}(z)$
end for
Finally, $\zeta_{n+1} := \varphi_n \circ \ldots \circ \varphi_1(z_0) \in \mathbb{R}$ and $\varphi_{n+1}(z) := -(\frac{z}{1-z/\zeta_{n+1}})^2$
Then $\psi(z) := \varphi_1^{-1} \circ \varphi_2^{-1} \circ \ldots \circ \varphi_{n+1}^{-1}(z)$ and $\psi^{-1}(z) := \varphi_{n+1} \circ \ldots \circ \varphi_2 \circ \varphi_1(z)$

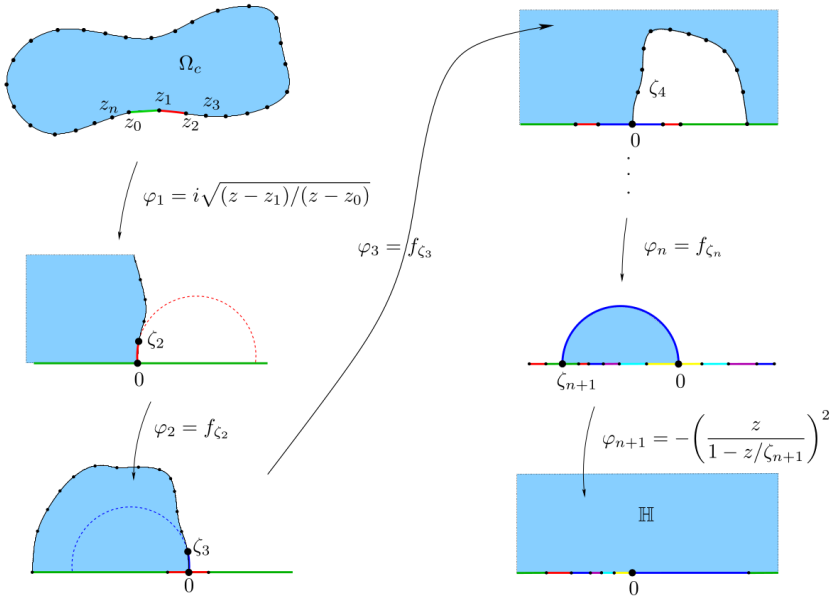

2.2.3 The Slit Algorithm

The above geodesic algorithm is only as accurate as the approximation of the boundary curve Γ by circular arcs between the points z_i. A more accurate version is given by the slit algorithm, which uses straight line segments instead of circular arcs. We therefore exchange the map f_a for a map $g_a : \mathbb{H} \setminus L \to \mathbb{H}$ where L is the line segment from 0 to $a \in \mathbb{H}$. This map does not have a closed form expression, but can be computed numerically using Newton's method.

2.2.4 The Zipper Algorithm

The approximation of Γ by circular arcs or straight line segments can be further improved by using circular arcs which meet Γ tangentially at the points z_i. Each arc is determined by the points z_i, z_{i+1} and z_{i+2}, hence we assume an even number of boundary points. The first arc is replaced by

$$\varphi_1(z) = \sqrt{\frac{(z-z_2)(z_1-z_2)}{(z-z_0)(z_1-z_2)}}.$$

At each subsequent step that circular arc through ζ_k and ζ_{k+1} is mapped onto a straight line segment by a Möbius transform, and then the Slit Algorithm is applied to unzip that segment. This yields a sort of "quadratic approximation" of $\partial\Omega$ instead of a linear one [MR06, page 8].

2.3 Conjugate Function Method

Hakula, Quach and Rasila [HQR13] presented a new method in 2010 which is based on solving the Laplace equation subject to Dirichlet-Neumann mixed-type boundary conditions by exploiting geometric properties of quadrilaterals.

Definition 13 ([HQR13, Definition 2.1])
A Jordan domain $\Omega \in \mathbb{C}$ with marked (positively ordered) points $z_1, z_2, z_3, z_4 \in \partial\Omega$ is called a **quadrilateral**, and is denoted by

$$Q = (\Omega; z_1, z_2, z_3, z_4).$$

Then there is a canonical conformal map of the quadrilateral Q onto a rectangle

$$R_h = (\Omega'; 1 + ih, ih, 0, 1)$$

with the vertices corresponding, where h defines the unique **modulus** of a quadrilateral Q. We write

$$M(Q) = h.$$

Note that the reciprocal identity holds:

$$M(Q)M(\tilde{Q}) = 1 \tag{14}$$

where $\tilde{Q} = (\Omega; z_2, z_3, z_4, z_1)$ is the **conjugate quadrilateral** of Q.

The method solves a PDE directly on the mesh on the entire domain $\mathbb{D}$ instead of only on the boundary in order to get the real part u of $\psi = u+iv$. The special feature then is that the conjugate function v is constructed by remarking that v solves the same PDE as u but with swapped boundary conditions. This second PDE is called the **dual problem**. Thus, the method essentially consists of solving two symmetric Laplace problems on the entire domain with different boundary conditions and combining their solutions to get ψ. The authors claim accuracy comparable with that of the standard Schwarz-Christoffel toolbox for both convex and non-convex quadrilaterals [HQR13, Figure 5].

2.4 Probabilistic Uniformization Method

In 2007, Binder, Braverman ans Yampolsky [BBY07] proposed a method for finding a conformal map using a random walks solver to the general Dirichlet problem. They conjectured an upper bound of polynomial space and time for an algorithm with precision $\frac{1}{n}$ pixels (for explicitly given $\partial\Omega$; quadratic if $\partial\Omega$ is given only approximately, via a so-called *oracle*, sort of a Dirac delta function). This method poses no constraints on the target region, but accuracy is unpredictable by definition.

2.5 Theodorsen's Method

For Ω star-shaped with regard to the origin, Theodorsen's method [Gai64, page 64] can be used to find the conformal mapping $\psi : \mathbb{D} \to \Omega$ satisfying the initial

conditions (1). Since Ω is star-shaped, the boundary Γ can be parametrized by the polar angle. Consequently, the boundary correspondence function $S(\varphi)$ defined in (3) becomes the angular function $\theta(\varphi)$. Theodorsen's integral equation is derived as follows: Note points on the unit circle are parametrised by $e^{i\varphi}$ while Γ can be parametrised by $\rho(\theta)e^{i\theta}$ for $\varphi, \theta \in [0, 2\pi]$ and $\rho(\theta) > 0$ the radius function of Γ (by star-shapedness of Ω). Thus, the problem reduces to relating φ and θ via a function $\theta(\phi)$. The trick is to introduce an auxiliary function involving a log, which allows to separate the real and imaginary part of the problem:

$$Re^{i\alpha} = \log(R) + i\alpha \tag{15}$$

However, log has a singularity at 0 which impedes direct application of the log as it contradicts with our normalization criterion on ψ (1). Thus the singularity is removed by dividing out z. This gives us the helper function

$$F(z) := \log(\frac{\psi(z)}{z}) = \log(\frac{\rho(\theta)e^{i\theta}}{e^{i\varphi}}) = \log(\rho(\theta)e^{i(\theta-\varphi)}) = \log(\rho(\theta)) + i(\theta - \varphi). \tag{16}$$

By the section on conjugate functions 5 the real and imaginary parts of this helper function are conjugate. Thus, we can relate them by

$$\theta - \varphi = K \log(\rho(\theta)) \tag{17}$$

which can be rewritten into Theodorsen's integral equation

$$\theta(\varphi) = \varphi + K \log(\rho(\theta(\varphi))). \tag{18}$$

The discretization as in [Gut83] is done by naming the difference between the boundary angle and the circle angle $Y := \theta - \varphi = \theta(\varphi) - \varphi$ the conjugate function of $X := \log(\rho(\theta)) = \log(|\eta(\varphi)|)$. Theodorsen's integral equation becomes the fixed point equation

$$y = \psi(y) := K_\Sigma \log(|\eta(\varphi + y)|) \tag{19}$$

where the equation is evaluated on a grid of $2N$ equidistant angles $\varphi_k = \frac{k\pi}{N}$ for $k = 0, \ldots, 2N-1$. Here, the vector y approximates the values of the continuous function $Y(\varphi)$ at these grid points, such that $y_k \approx Y(\varphi_k)$. The product y can be computed efficiently using FFT (see chapter 1.3). In case of Γ not being smooth, Theodorsen's method becomes inaccurate [Gut83]. It also theoretically needs Ω to be star-shaped in order to converge [Weg78], since otherwise the radius function $\rho(\theta)$ becomes multivalued causing numerical failure, but has the advantage of being an easily computable fixed point equation if star-shaped. In practice, the star-shape requirement can also be relaxed by smoothing the boundary curve first using preliminary maps [Gut83].

2.6 Amano's Method of Fundamental Solutions

A potential theoretic formulation of the conformal mapping problem leads to a Fredholm integral equation of the first kind, known as Symm's integral equation, which has a kernel with logarithmic singularity. Unlike Fredholm integral

equations of the second kind like Theodorsen's equation, where the singularity of the kernel creates numerical instabilities, Symm's equation is easily solvable by numerical methods [Kyt98, Chapter 9.1]. One of these is Amano's method. Conceptually, a pair of conjugate harmonic functions are expressed by a complex logarithmic potential, and the mapping problems are reduced to singular Fredholm integral equations of the first kind. Gaier [Gai64] mathematically studied Symm's integral equation and proved the existence and uniqueness of the solution. These methods need $\mathcal{O}(N^3)$ operations if the boundary is discretized at N points. Henrici showed that complexity of $\mathcal{O}(N^2 \log N)$ can be achieved by using FFTs [Hen86].

Definition 14 ([Ama98, § 4])
In two dimensions, the Laplace equation has a fundamental solution of the form $\log(r)$ where $r = |z - \zeta_k|$ is the modulus of the vector from any point z on the region to the boundary point ζ_k, $k \in N$. This function $\log(|z - \zeta_k|)$ is called the **logarithmic potential**.

A potential theoretic formulation of the Dirichlet problem (4) leads to a Fredholm integral equation of the first kind called **Symm's equation**

$$\int_\Gamma \log|z - \zeta| \mu(\zeta) d\zeta = -\log|z| \quad \text{for } z \in \Omega, \zeta \in \Gamma \tag{20}$$

which has a kernel with logarithmic singularity. In this context, the conformal mapping problem reduces to finding a suitable source density function $\mu(z) = g(z) + ih(z)$ on the boundary Γ where g and h are conjugate and g satisfies

$$\begin{array}{rl} \nabla^2 g(z) = 0 & z \in \Omega \\ g(z) = -\frac{1}{2}\log|z\bar{z}| & z \in \Gamma. \end{array} \tag{21}$$

It is more easily solvable by numerical methods than Fredholm integral equations of the second kind, where the kernel might have singularities near the boundary [Kyt98, Chapter 9].

This is used in the so-called Charge Simulation Method which Amano's Method is based on.

2.6.1 Algorithm

The charge simulation method approximates the solution of the Laplace equation by a linear combination of fundamental solutions placed at so-called charge points outside the domain [Ama98] by

$$g(z) = \sum_{k=1}^{N} Q_k log(|z - \zeta_k|), \tag{22}$$

where $\zeta_1, \ldots, \zeta_N \notin \overline{\Omega}$ are called **charge points** and placed outside the domain. The unknown constants $Q_1, \ldots, Q_N$ are called **charges** and determined to satisfy the boundary condition at the **collocation points** $z_1, \ldots, z_N$ (fixed check

points on the boundary $\partial\Omega$). Hence, Q_k are found by plugging in the collocation points into the below **collocation condition** and solving the linear system:

$$\eta(z_i) = \sum_{k=1}^{N} Q_k log(|z_i - \zeta_k|), \quad i = 1, 2, ..., N. \tag{23}$$

Then the conformal map $\psi(z) = g(z) + ih(z)$ is constructed, where $h(z)$ is the harmonic conjugate of $g(z)$. If the boundary is analytic, this method can be shown to have exponential accuracy i.e. exponentially small error in the number of collocation points [Ama98].

2.7 Method of Alternating Projections

Various methods for numerical construction of ψ essentially construct two sequences of functions, one of normalized analytic functions on the disk and one mapping the boundary of $\mathbb{D}$ to the boundary Γ. The method of alternating projections uses both these sequences and alternates between them to find ψ [Weg89]. Before giving the geometrical intuition we start by introducing the necessary function spaces.

2.7.1 Sobolev Spaces

Let $L^2([0, 2\pi])$ be the space of all 2π-periodic complex functions f which are square integrable over $[0, 2\pi]$ equipped with the inner product

$$(f, g)_2 = \frac{1}{2\pi} Re \int_0^{2\pi} f(t)\overline{g(t)}dt. \tag{24}$$

Definition 15 ([Wik25f])
The **Sobolev space** W is defined as the space of all absolutely continuous functions $f \in L^2$ such that the derivative f' exists and is also in L^2. The inner product on W is defined as

$$(f, g)_W = (f, g)_2 + (f', g')_2.$$

This is a Hilbert space over $\mathbb{R}$. The subspaces of real functions are denoted $L^2_{\mathbb{R}}$ and $W_{\mathbb{R}}$ respectively. Note that we can orthogonally decompose W into the direct sum of the subspaces $W = W^+ \oplus W^-$ [Weg89] where $f \in L^2$ is decomposed as follows into its Fourier series:

$$f(t) = \sum_{n=-\infty}^{\infty} a_n e^{int} = \underbrace{\sum_{-\infty}^{0} a_n e^{int} + i(\mathrm{Im}(a_1))e^{it}}_{=:f^- \in W^-} + \underbrace{(\mathrm{Re}(a_1))e^{it} + \sum_{n=2}^{\infty} a_n e^{int}}_{=:f^+ \in W^+}.$$

This allows for $\psi'(0) = a_1 \in \mathbb{R}_{>0}$ when projecting onto W^+ later, as required by (1). Note that linear spaces are convex, as convex combinations of functions

are still in the space. In view of this, the conformal mapping ψ we are looking for can be expressed as follows:

$$\psi(t) = \eta(t + \hat{U}(t)) \in W^+ \quad \forall t. \tag{25}$$

By (3) $\hat{U}$ exists and by the implicit function theorem 1.8 it is continuously differentiable, hence $\hat{U} \in W_{\mathbb{R}}$. Next, define the differentiable manifold of functions mapping the boundary of the disk to the boundary Γ as

$$M := \{\eta(t + U(t)) : U \in W_{\mathbb{R}}\}. \tag{26}$$

Thus, $\psi \in M \cap W^+$ where

$$\begin{aligned} M &:= \{f : \partial\mathbb{D} \to \Gamma\} \\ W^+ &:= \{f \text{ analytic on } \mathbb{D}\}. \end{aligned} \tag{27}$$

Note that a manifold is not convex in general; In the algorithm [Weg89, §3] the mapping in the intersection is found by approximating it first on the tangent space at each interation-specific point of the manifold instead. This can be understood as a local linearisation of M.

2.7.2 Geometric Derivation (Alternating Projections)

For two closed convex sets P, Q in a Hilbert space H, the method of alternating projections constructs a sequence $(x_n)_n$ as follows: Starting from an arbitrary point $x_0 \in H$, we define

$$x_{n+1} := \begin{cases} \Pi_P(x_n) & n \equiv 0 (\text{mod } 2) \\ \Pi_Q(x_n) & n \equiv 1 (\text{mod } 2) \end{cases}$$

where $\Pi_P(z) = \min_{x \in P} \|x - z\|^2$ and $\Pi_Q(z) = \min_{x \in Q} \|x - z\|^2$ denote the orthogonal projections onto the sets P and Q respectively. It can be shown that the sequence $(x_n)_n$ converges in the respectively used norm to a point tuple $(x*, y*)$ satisfying

$$\begin{cases} x* = \Pi_P(y*), \\ y* = \Pi_Q(x*), \\ d_H(x*, y*) = \min_{(x,y) \in P \times Q} \|x - y\|^2 \end{cases}$$

In particular, $x* = y*$ if $P \cap Q \neq \emptyset$.

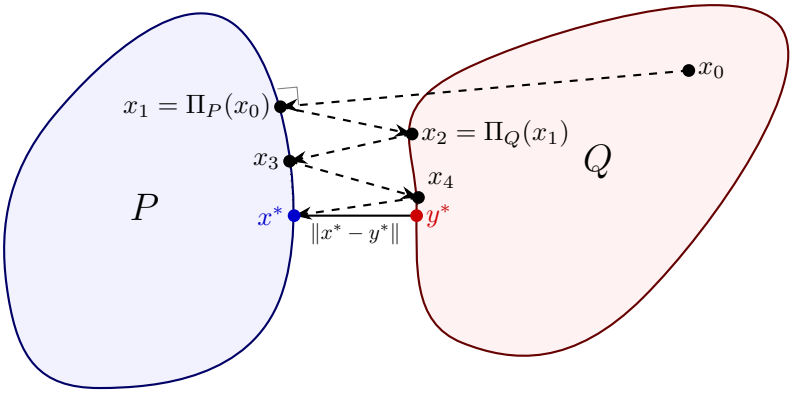

This exact idea is applied to function spaces using $x_0 = U_0 \in M, P = W^+$ and $Q = T_k$ the tangent space approximating M at the current iteration.

Algorithm 2 AP-Method

Start with a function $U_0 \in W_{\mathbb{R}}$.
Given U_k for $k \geq 0$,
for $n = 1, 0, -1, \ldots$ **do**
$a_n = \frac{1}{2\pi} \int_0^{2\pi} \eta(t + U_k(t)) e^{-int} dt$ [Calculate Fourier coefficients]
end for
$U_{k+1}(t) := U_k(t) - \mathrm{Re} \frac{i(\mathrm{Im}(a_1))e^{it} + \sum_{n=-\infty}^{0} a_n e^{int}}{\dot{\eta}(t+U_k(t))}$ [Calculate the new iterate]

2.7.3 Alternating Projections with Overrelaxation (OAP)

The OAP method is a variant of the AP method which introduces an overrelaxation parameter to speed up convergence [Weg89, § 4]. The algorithm is the same except for a constant factor in the definition of U_{k+1}. This factor decreases the number of outer iterations, which in our case are the iterations indexed by k, performed until convergence. The complexity of each individual iteration remains of order $\mathcal{O}(N \log N)$ due to the FFT computation of the Fourier coefficients.

2.8 Wegmann's Method

The projection onto the tangent space described above is analytically equivalent to a linearization of the boundary value problem. Wegmann [Weg78] showed that the update shift $U_k(t)$ is the solution to the linearized equation below. Given η the differentiable parametrization of Γ with $\dot{\eta}(s) \neq 0 \ \forall s$, we construct the conformal mapping by iterated correction of an initial guess S as follows.

Assume that the approximation for ψ after k steps be given by $\psi_k(\zeta) = \eta(S_k(\zeta))$.

$$\partial\mathbb{D} \xrightarrow{S} [0, 2\pi] \xrightarrow{\eta} \Gamma$$
$$\psi$$

We improve the approximation by moving the points along their tangents towards the boundary curve, i.e. by finding a correction function $U_k : \partial\mathbb{D} \to [0, 2\pi]$ such that

$$\eta(S_k(\zeta)) + U_k(\zeta)\dot{\eta}(S_k(\zeta)) = \psi_{k+1}(\zeta) \tag{28}$$

where ψ_{k+1} is an analytic approximation for ψ on $\overline{\Omega}$. Note that ψ_{k+1} does not generally take values on Γ. The above equation (28) has two unknowns, U_k and ψ_{k+1}, which makes it a Riemann-Hilbert Problem. By the Riemann Mapping Theorem, it admits a unique solution only if we fix the mapping normalization. We therefore require that a specific boundary point z_0 corresponds to the target parameter s_0 (where $\eta(s_0) = c_0$). A direct coordinate constraint $\psi_{k+1}(z_0) = c_0$ is geometrically impossible because $\psi_{k+1}(z_0)$ is constrained to the tangent vector, while c_0 lies on the curve Γ. Therefore, the normalization condition is transferred to the parameter space. We force the updated parameter function to satisfy $S_{k+1}(z_0) = s_0$, which directly yields the necessary boundary condition for U_k [Weg78, Equation 2.4a]:

$$U_k(z_0) = s_0 - S_k(z_0). \tag{29}$$

To find U_k, equation (28) is rewritten into [Weg78, Equation 3.4]:

$$\mathrm{Re}\left(\frac{\psi_{k+1}}{i\dot{\eta}(S_k(\zeta))}\right) = \mathrm{Im}\left(\frac{\eta(S_k(\zeta))}{\dot{\eta}(S_k(\zeta))}\right). \tag{30}$$

This eliminates U_k (since it is real-valued) and yields a boundary value problem for ψ_{k+1} which can be solved using the operator K defined in 1.3. This is done via FFT (see 2.8.1). Subsequently, U_k is recovered by rearranging equation (28).

Finally, we get an approximation for the parametrization S by

$$S_{k+1}(\zeta) := S_k(\zeta) + U_k(\zeta) \tag{31}$$

which can be understood as "new guess equals last guess plus some correction".

2.8.1 Implementation

Since we assume ψ to map from the unit disk $\mathbb{D}$, the integral equations can be explicitly solved by discretization and trigonometric interpolation [Weg78, §5]: Take $N = 2n$ equidistant points $\zeta_k = e^{i\theta_k}$ on the boundary of the disk, where

$$\theta_k = \theta_0 + \frac{\pi k}{N}, \quad k \in [N-1]$$

Algorithm 3 Wegmann's Method

Input: Target boundary $\eta : [0, 2\pi] \to \mathbb{C}$, anchor points $z_0 \in \partial\mathbb{D}, s_0 \in [0, 2\pi]$.
Initialize: $S_0(\zeta) = \arg(\zeta)$ (Identity) or guess satisfying $S_0(z_0) = s_0$.
while not converged **do**
    // 1. Evaluate current boundary geometry
    $f_k(\zeta) := \eta(S_k(\zeta))$
    $g_k(\zeta) := \dot{\eta}(S_k(\zeta))$
    // 2. Solve Riemann-Hilbert Problem with anchoring
    Find analytic function ψ_{k+1} on $\mathbb{D}$ satisfying:

$$\mathrm{Re}\left(\frac{\psi_{k+1}(\zeta)}{i g_k(\zeta)}\right) = \mathrm{Im}\left(\frac{f_k(\zeta)}{g_k(\zeta)}\right) \quad \forall \zeta \in \partial\mathbb{D}$$

    subject to the constraint:

$$\mathrm{Re}\left(\frac{\psi_{k+1}(z_0) - f_k(z_0)}{g_k(z_0)}\right) = s_0 - S_k(z_0)$$

    // 3. Compute correction and update
    $U_k(\zeta) := \mathrm{Re}\left(\frac{\psi_{k+1}(\zeta) - f_k(\zeta)}{g_k(\zeta)}\right)$
    $S_{k+1}(\zeta) := S_k(\zeta) + U_k(\zeta)$
end while

and write the integrals in terms of their Fourier transform

$$F(z) = \frac{1}{2\pi i} \int \frac{\sigma_n(\zeta)}{\zeta - z} d\zeta \tag{32}$$

where

$$\sigma_n(\zeta_k) = \sum_{i=-n}^{n} c_i \zeta_k^i.$$

This $\sigma_n \mapsto F$ can be computed fast ($\in \mathcal{O}(N \log N)$) via FFT.

Note that this is a Newton method and thus only guaranteed to converge locally due to the linearisation of the boundary. Hence why a "good" (close enough) initial guess is vital for numerical stability. In practice, for Ω far from circular, a homotopy method could probably be adopted, where each solution for a slightly deformed circle is used as initial guess for the next deformation until the target region is reached. Unlike the AP Method, which uses a fixed projection to find the next iterate, Wegmann's Method leverages the exact geometry of the boundary curve via θ, which yields quadratic convergence since the error decreases much faster [Weg78, Theorem 4].

2.9 Comparison

We can directly rule out some of the options due to our project constraints: First we note that Schwarz-Christoffel only works on polygons and Theodorsen's method is restricted to star-shaped regions. Since we want to be able to work with more general shapes of Ω, we disregard these two methods.

We refrain from using probabilistic methods due to their inherent randomness and the difficulty of guaranteeing a certain accuracy, but it is worthwile noting that this is a good choice in cases where the boundary is so rough/ irregular that deterministic methods fail. Since we are given a smooth boundary of the target domain, we can opt for a more accurate method.

The Zipper method is very well implementable and robust (it can handle rough boundaries including fractals), but there is a small caveat to be aware of for the efficient point evaluations. Since the Zipper method essentially constructs ψ as a composition of many maps, the derivative is numerically expensive to compute (chain rule). Also, trying a finite differences approach is slow and potentially numerically unstable, but there is hope in a technique called Forward Automatic Differentiation which is both exact and efficient [Wik25a].

The Conjugate Function Method contains a very astute idea mathematically, but its implementation is not very interesting beyond *hp*-FEM for which there already are powerful libraries, so there would not be much value in implementing a rudimentary FEM solver given the scope of this thesis.

Amano's Method of Fundamental Solutions seems good for fast (linear time) point-evaluations of ψ as well as its derivative as it is a sum of simple fractions and all the singularities (charge points) are placed strictly outside the region. However, we cannot directly use our Fourier parametrization nor our mesh in this method, so it will probably not be the best choice for our specific problem. Note also that the accuracy and convergence of this method depend on the right choice of charge points.

Lastly, Wegmann's Method and the Method of Alternating Projections both use the boundary parametrization in its Fourier series form. In both cases, the output is an interpolating polynomial, allowing for efficient point evaluations of ψ and $D\psi$ [Weg84]. The AP Method is one of the simplest and most robust methods for conformal mapping. However, it is not very accurate for reasonably sized grids, and converges only linearly [Weg05, Chapter 4.2]. In contrast, Newton's Method converges quadratically for analytic boundaries (as is known for Newton methods) and superlinear ($\in \mathcal{O}(N^{1+\mu})$) for $\eta \in C^{2+\mu}$ but depends on a "good enough" initial guess for the boundary correspondence function (3) [Weg78, § 4], [Weg89, page 292], [Weg84].

Hence, both Zipper, AP and Wegmann's methods seem suitable for our problem, but Wegmann's Method is most accurate with fastest convergence while seemingly the most interesting to implement. The Zipper method is also very appealing due to its robustness, but since we are given a smooth boundary and want high accuracy, we can afford to use a method that is less robust but more accurate. We will therefore opt for implementing Wegmann's Method.

Table 1: Comparison of Numerical Conformal Mapping Methods

Method	Ω **Shape**	**Runtime**	**Input**	**Output**	**Advantages**	**Disadvantages**
Schwarz-Christoffel	Polygon	$\mathcal{O}(N^3)$ (parameter problem)	Polygon vertices z_k and angles θ_k	Integral parameters: prevertices v_k, C	Exact angle preservation at corner singularities; Handles unbounded & periodic domains.	Restricted to polygons; Crowding (resolution loss); Slow
Theodorsen	Star-shaped	$\mathcal{O}(N \log N)$	Radial function $\rho(\theta)$	Boundary correspondence $\theta(\phi)$	Fast fixed-point iteration; Efficient FFT implementation.	Restricted to star-shaped regions; Fails/Inaccurate for non-smooth boundaries or shapes far from $\mathbb{D}$.
Zipper (Geodesic)	General Jordan incl. Fractals	Fast, Dep. only on N but not on shape	Boundary points $\{z_i\}_{i\in[N]}$	Composition of elementary maps	Robust (handles fractals); Finds inverse simultaneously.	Expensive derivative computation (chain rule); Only approximates Γ.
Conjugate Function	General, incl. sharp corners/ cusps	Dep. on mesh, slower than SC on polygons	Boundary & 4 marked vertices	Conformal modulus h & u, v potentials s.t. $\psi(z) = u(z) + ih(z)$	Exponential convergence using hp-FEM; Works on rough boundaries; Numerical stability thanks to dual BVP	Point evaluation expensive (searching mesh)
Probabilistic	General, incl. Rough/ Fractals	Polynomial	Oracle / Boundary (pixel list)	Random Walk approx.	Works on rough boundaries where deterministic methods fail.	Slow convergence; Inherent randomness; Difficult to guarantee accuracy.
Amano	Analytic	$\mathcal{O}(N^3)$	Collocation points z_i	Lin. comb. of log potentials	Fast linear point/derivative evaluation; Exponential accuracy; Simple implementation.	Cannot use Fourier param. or mesh; Sensitive to charge point placement.
Alternating Projections	Smooth	$\mathcal{O}(N \log N)$ per iter.: FFT	Fourier Series of η	Analytic Interpolating Polynomial for Boundary Corresp. Fct	Efficient point evaluation; Robust (less dependent than Wegmann's on initial guess).	Linear (slow) convergence; Requires smooth boundary; Approximative Solution (inaccurate).
Wegmann	Smooth	$\mathcal{O}(N \log N)$ per iter.: FFT	Fourier Series of η	Analytic Interpolating Polynomial for Boundary Corresp. Fct	Quadratic (fast) convergence; High accuracy (FFT); Efficient point evaluation.	Requires good initial guess (local convergence); Requires smooth boundary.

3 Proposed Method

3.1 Choice/ Justification

3.2 Implementation

- WHAT FORMAT DOES THE MESH HAVE I WILL BE GIVEN - Separate modules for boundary parameterization, mapping computation, Jacobian eval, and mesh transformation - plot original vs. mapped grids (e.g., Matplotlib quiver for Jacobians) to spot issues early.

3.3 Numerical Experiments/ Testing

check angle preservation (e.g., via dot products on mapped vectors) and scale factors ($det(D\Phi) > 0$, $|\frac{\partial \Phi}{\partial z}|$ constant in theory). - Test suite: Use known exact mappings (e.g., disk to square via Schwarz-Christoffel) for error metrics (L2 norm on boundary points). - Metrics: Runtime for N points, mesh quality post-mapping (e.g., min/max angles in triangles, shape regularity ratio). - Real-world applicability: Apply to a sample FEM problem (e.g., Poisson equation on Ω) and compare accuracy/speed vs. uniform mesh. - Robustness: Vary boundary complexity (smooth vs. corners), noise in Fourier coeffs, mesh resolutions. - Debugging: Use assertions for bijectivity (e.g., check injectivity numerically) - Error handling - what happens with degenerate inputs?

3.4 Results

4 TO DO

- zuerst überlegen, dann programm schreiben - geeignete datenstrukturen? - modularer code! - gleichzeitig tests schreiben wie code, für die modularen fkt und auch für gesamtalgo um korrektheit zu prüfen - if there is a known mapping e.g. from square to disk given as an explicit formula, use this for testing of correctness - speziell konvergenzaussagen related to metrik ("abstand zum limes") spezifizieren und genau zitieren - auf papier, implementieren, testen, dann melden sonst wenns probleme gibt

- chebfun.org

future work: maybe mention more niche methods which were not covered for time reasons

5 Documentation and Implementation

5.1 Testing (again?)

VALIDATION AGAINST THE SCHWARZ-CHRISTOFFEL TOOLBOX!

References

[Ama98] Kaname Amano. A charge simulation method for numerical conformal mapping onto circular and radial slit domains. *SIAM Journal on Scientific Computing*, 19(4):1169–1187, 1998.

[Ban08] Lehel Banjai. Revisiting the crowding phenomenon in schwarz–christoffel mapping. *SIAM Journal on Scientific Computing*, 30(2):618–636, 2008.

[BBY07] Ilia Binder, Mark Braverman, and Michael Yampolsky. On computational complexity of riemann mapping, 2007.

[Bro90] Philip Raymond Brown. *The use of the Schwarz-Christoffel transformation in finite element mesh generation*. Phd, University of Leicester, 1990.

[CR25] René E. Castillo and Edixon M. Rojas. Revisiting the hilbert transform of periodic functions. *Mathematische Semesterberichte*, 72:29–49, 2025.

[DeL94] Thomas K. DeLillo. The accuracy of numerical conformal mapping methods: A survey of examples and results. *SIAM Journal on Numerical Analysis*, 31(3):788–812, 1994.

[EW22] Manfred Einsiedler and Andreas Wieser. Analysis i und ii. Vorlesungsskript 2021/2022, 2022.

[Gai64] Dieter Gaier. *Konstruktive Methoden der konformen Abbildung*, volume 3 of *Springer Tracts in Natural Philosophy / Ergebnisse der angewandten Mathematik*. Springer-Verlag, Berlin, Göttingen, Heidelberg, 1964.

[Gut83] Martin H. Gutknecht. Numerical experiments on solving theodorsen's integral equation for conformal maps with the fast fourier transform and various nonlinear iterative methods. *SIAM Journal on Scientific and Statistical Computing*, 4(1):1–30, 1983.

[Hen86] Peter Henrici, editor. *Applied and computational complex analysis. Vol. 3: discrete Fourier analysis—Cauchy integrals—construction of conformal maps—univalent functions*. John Wiley & Sons, Inc., USA, 1986.

[Hip23] Ralf Hiptmair. Numerical methods for partial differential equations. Lecture Notes, Seminar for Applied Mathematics, ETH Zurich, 2023.

[HQR13] Harri Hakula, Tri Quach, and Antti Rasila. Conjugate function method for numerical conformal mappings. *Journal of Computational and Applied Mathematics*, 237(1):340–353, January 2013.

[Kyt98] Prem K. Kythe. *Symm's Integral Equation*, pages 237–268. Birkhäuser Boston, Boston, MA, 1998.

[MR06] Donald E. Marshall and Steffen Rohde. Convergence of the zipper algorithm for conformal mapping, 2006.

[Pom92] Christian Pommerenke. *Boundary Behaviour of Conformal Maps*, volume 299 of *Grundlehren der mathematischen Wissenschaften*. Springer-Verlag, Berlin, 1992.

[SS03] Elias M. Stein and Rami. Shakarchi. *Complex analysis*. Princeton lectures in analysis ; 2. Princeton University Press, Princeton, N.J, 2003.

[Tre80] Lloyd N. Trefethen. Numerical computation of the schwarz–christoffel transformation. *SIAM Journal on Scientific and Statistical Computing*, 1(1):82–102, 1980.

[Wec19] F Wechsung. *Shape optimisation and robust solvers for incompressible flow*. PhD thesis, University of Oxford, 2019.

[Weg78] Rudolf Wegmann. Ein iterationsverfahren zur konformen abbildung. *Numerische Mathematik*, 30(4):453–466, 1978.

[Weg84] Rudolf Wegmann. Convergence proofs and error estimates for an iterative method for conformal mapping. *Numerische Mathematik*, 44:435–461, 1984.

[Weg89] Rudolf Wegmann. Conformal mapping by the method of alternating projections. *Numerische Mathematik*, 56:291–307, 1989.

[Weg05] Rudolf Wegmann. Chapter 9 - methods for numerical conformal mapping. In R. Kühnau, editor, *Geometric Function Theory*, volume 2 of *Handbook of Complex Analysis*, pages 351–477. North-Holland, 2005.

[Wik25a] Wikipedia contributors. Automatic differentiation — Wikipedia, the free encyclopedia. `https://en.wikipedia.org/w/index.php?title=Automatic_differentiation&oldid=1320248234`, 2025. [Online; accessed 14-November-2025].

[Wik25b] Wikipedia contributors. Fredholm integral equation — Wikipedia, the free encyclopedia. `https://en.wikipedia.org/w/index.php?title=Fredholm_integral_equation&oldid=1314003753`, 2025. [Online; accessed 7-December-2025].

[Wik25c] Wikipedia contributors. Hurwitz's theorem (complex analysis) — Wikipedia, the free encyclopedia. `https://en.wikipedia.org/w/index.php?title=Hurwitz%27s_theorem_(complex_analysis)&oldid=1321322619`, 2025. [Online; accessed 7-December-2025].

[Wik25d] Wikipedia contributors. Möbius transformation — Wikipedia, the free encyclopedia. https://en.wikipedia.org/w/index.php?title=M%C3%B6bius_transformation&oldid=1323948782, 2025. [Online; accessed 8-December-2025].

[Wik25e] Wikipedia contributors. Polygon — Wikipedia, the free encyclopedia. https://en.wikipedia.org/w/index.php?title=Polygon&oldid=1320067726, 2025. [Online; accessed 8-December-2025].

[Wik25f] Wikipedia contributors. Sobolev space — Wikipedia, the free encyclopedia. https://en.wikipedia.org/w/index.php?title=Sobolev_space&oldid=1324240611, 2025. [Online; accessed 8-December-2025].